

*Biochemistry*. Author manuscript; available in PMC 2010 November 3.

Published in final edited form as:

Biochemistry. 2009 November 3; 48(43): 10405-10415. doi:10.1021/bi900523q.

# Surface Plasmon Resonance Binding Kinetics of Alzheimer's Disease Amyloid β Peptide Capturing- and Plaque Binding-Monoclonal Antibodies<sup>†</sup>

Muthu Ramakrishnan $^{\ddagger}$ , Karunya K. Kandimalla $^{\ddagger,\S}$ , Thomas M. Wengenack $^{\ddagger}$ , Kyle G. Howell $^{\ddagger}$ , and Joseph F. Poduslo $^{\ddagger,*}$ 

<sup>‡</sup>Molecular Neurobiology Laboratory, Departments of Neurology, Neuroscience, and Biochemistry/ Molecular Biology, Mayo Clinic College of Medicine, Rochester, MN

§College of Pharmacy and Pharmaceutical Sciences, Florida A&M University, Tallahassee, FL

### **Abstract**

Several different monoclonal antibodies (mAbs) have been actively developed in the field of Alzheimer's disease (AD) for basic science and clinical applications; however, the binding kinetics of many of the mAbs with the  $\beta$ -amyloid peptides (A $\beta$ ) are poorly understood. A panel of mAbs with different Aβ recognition sites, including our plaque binding antibody (IgG4.1), a peptide capturing antibody (11A50), and two classical mAbs (6E10 and 4G8) used for immunohistochemistry, were chosen to characterize their binding kinetics to monomeric and fibrillar forms of Aβ40 using surface plasmon resonance and their amyloid plaque binding ability in AD mouse brain sections using immunohistochemistry. The plaque binding antibody (IgG4.1) with epitope specificity of Aβ(2-10) showed a weaker affinity (512 nM) to monomeric Aβ40 but higher affinity (1.5 nM) to Aβ40 fibrils and labeled dense core plaques better than 6E10 by immunohistochemistry. The peptide capturing antibody (11A50) showed preferential affinity (32.5 nM) to monomeric Aβ40, but did not bind to Aβ40 fibrils, whereas antibodies 6E10 and 4G8 had moderate affinity to monomeric Aβ40 (22.3 and 30.1 nM, respectively). 4G8, which labels diffuse plaques better than 6E10, had a higher association rate constant than 6E10 but showed similar association and dissociation kinetics compared to 11A50. Enzymatic digestion of IgG4.1 to the F(ab')<sub>2</sub>4.1 fragments or their polyamine-modified derivatives that enhance blood brain barrier permeability did not affect the kinetic properties of the antigen binding site. These differences in kinetic binding to monomeric and fibrillar Aβ among various antibodies could be utilized to distinguish mAbs that might be useful for immunotherapy or amyloid plaque imaging versus those that could be utilized for bioanalytical techniques.

### **Keywords**

Alzheimer's disease; surface plasmon resonance; peptide capturing antibodies; plaque labeling antibodies; immunotherapy; antibody fragments

Alzheimer's disease (AD) is an incurable neurodegenerative disease that affects predominantly the aged population. While the disease pathology is not well understood, it is believed that the

<sup>†</sup>Support was provided by Minnesota Partnership for Biotechnology and Medical Genomics and the Neuroscience Cores for MR Studies of the Brain from NINDS (NS057091).

<sup>\*</sup>Corresponding Author: Joseph F. Poduslo, Ph.D. Departments of Neurology, Neuroscience, and Biochemistry/Molecular Biology Mayo Clinic College of Medicine 200 First Street SW Rochester, MN 55905 Phone: 507 284 1784 FAX: 507 284 3383 poduslo.joseph@mayo.edu.

disease is associated with the accumulation of toxic amyloid peptides ( $A\beta$ ) preferentially in the brain, which aggregate to form amyloid plaques and cerebrovascular deposits (1). In the monomeric form,  $A\beta$  peptide is randomly oriented without any ordered structure, but in the fibrillar form it shows several different polymorphic structures. (2-4). In the AD patient brain, these polymorphic  $A\beta$  fibrils are associated with dystrophic neurites, microglia, and astrocytes which are called neuritic amyloid plaques or with diffuse plaques which are the precursor forms of dense core plaques without dystrophic neurites. These diffuse plaques are not only present in AD patients but are also found in healthy aged humans free of any signs of dementia (1). While the mechanism of neuronal dysfunction is still not clear, it is widely believed that a particular form of amyloid protein assembly could impair memory in AD patients (5),(6).  $A\beta$  peptide, therefore, is a primary diagnostic and therapeutic target for AD.

It was reported previously that peripheral administration of mAbs in AD transgenic mice showed efficacy in reducing the brain amyloid plaque burden (7). As a result, many different monoclonal antibodies have been developed to target AB peptides and are in different stages of clinical trials for immunotherapy in AD patients by major biopharmaceutical companies with the emphasis of clearing the extracellular A $\beta$  plaque deposits in AD patients and promoting behavioral improvements (8,9). However, fundamental differences have been observed with these mAbs, such as recognition of the Aβ antigen, affinity to Aβ, and the mechanism of action. Bard et al. (7) reported that an N-terminal antibody (3D6), which supposedly crosses the blood brain barrier (BBB), clears parenchymal amyloid deposits presumably via microglial phagocytosis. DeMattos et al. (10) showed that a high affinity Aβ peptide capturing antibody (m266), which targets the central domain of Aß but lacks binding to plaques reduces A $\beta$  deposits from the brain by supposedly sequestering A $\beta$  to the plasma and thereby altering the Aß equilibrium between brain and circulating plasma. Recently, Seubert et al. (11) reported that this peptide capturing antibody (m266) is not efficient in clearing plaques as it also increases cerebrovascular amyloidosis, whereas a plaque-binding antibody, 3D6, is highly effective in reducing the plaque load present in the brain and cerebrovasculature.

Assessment of the therapeutic potential of anti-A $\beta$  antibodies largely depends on expensive *in vivo* pharmacokinetic and pharmacodynamic experiments. Moreover, it is difficult to screen and define the required biochemical and biophysical properties of a potential antibody for immunotherapy through *in vivo* studies. In addition, most of these antibodies are not commercially available to researchers so that systematic studies can be conducted. Those antibodies that are commercially available for investigational purposes are also cost prohibitive to conduct immunotherapeutic preclinical trials. IgG4.1 is our own monoclonal antibody raised against fibrillar human A $\beta$ 42 peptide developed for therapeutic and diagnostic purposes for AD. Recently, we have demonstrated that the polyamine (p) modified F(ab')<sub>2</sub> fragment of IgG4.1 had increased BBB permeability by ~25 and ~50 fold compared to the native IgG4.1 or F(ab')<sub>2</sub>4.1 and successfully targeted amyloid plaques after i.v. administration (12,13). Obviously, increasing the delivery payload across the BBB even by a small fraction could have a great therapeutic impact, since only about 0.1 -1 % of therapeutic antibodies are present in CNS after the immunization. Compared to insulin, which undergoes receptor mediated transcytosis, antibodies have nearly a 240 -fold lower BBB permeability (14).

Apart from immunotherapy, monoclonal antibodies are also used extensively in basic science for bioanalytical purposes, such as ELISA, to quantify A $\beta$  peptides in tissues, plasma, and cerebrospinal fluid (15-17), and also to develop novel immune conjugates for diagnostic imaging (12,18). In this study, we have chosen a set of mAbs against A $\beta$  peptides developed for Alzheimer's disease for different purposes: 1) a peptide capturing antibody which captures soluble A $\beta$  for bioanalytical techniques; 2) two mAbs for labeling diffuse and dense core amyloid plaques in tissue sections for immunohistochemistry techniques; and 3) a plaque

binding antibody for diagnostic as well as therapeutic purposes. We characterized the binding properties of these mAbs to monomeric and fibrillar human A $\beta$ 40 using surface plasmon resonance (SPR) biosensor technology and their ability to bind diffuse and dense core plaques present in AD mouse brain sections using immunohistochemistry. We show that these mAbs have some fundamental differences in their biophysical interactions with different structures of monomeric and fibrillar A $\beta$ 40 and thus manifest different binding kinetics. The results are discussed in the context of choosing and developing these mAbs for specific needs for AD research. We have also studied the epitope mapping of IgG4.1 and demonstrated that the enzyme digestion of native IgG4.1 to F(ab')<sub>2</sub>4.1 preserved the antigen binding regions.

### **MATERIALS AND METHODS**

### **Animals**

Hemizygous transgenic mice (mouse strain: C57B6/SJL; I.D. No. Tg2576) expressing mutant human amyloid precursor protein (APP695) (19) were bred in our mice colony at Mayo. These transgenic mice have been shown to exhibit parenchymal amyloid deposits by 12 months of age (20). The animals were housed in a virus-free, light and temperature controlled barrier environment. They were provided with free access to food and water. All procedures with animals were in strict accordance with National Institutes of Health Guide for the Care and Use of Laboratory animals and were approved by the Mayo Institutional Animal Care and Use Committee.

### Preparation of Monomeric and Fibrillar Aβ40

Aβ40 peptide was obtained from Mayo Peptide Core Facility (Rochester, MN) in lyophilized form. The preparation of monomeric Aβ40 followed the procedures described by Bitan et al. (21) and Nichols et al. (22). The monomeric  $A\beta 40$  peptide was purified further using the method described by Nichols et al. (22). Briefly, the monomeric Aβ40 was purified from lyophilized Aβ40 at a concentration of 4 μg/μl in HBS-EP buffer (0.01 M HEPES, pH 7.4, 0.15 M NaCl, 3 mM EDTA, 0.005% P20) and bath sonicated for 40 seconds to get clear solution. The sample was spun at 14000 rpm for 20 min and filtered through 0.2 µm to remove any large aggregates before injecting 200 µl of sample to Superdex size exclusion column connected to an FPLC system. The concentration of purified monomeric Aβ40 was determined by measuring its absorbance at 280 nm and using the absorption coefficient of 1490. The concentration of 4 µg/  $\mu$ l of A $\beta$ 40 was used for the consistent preparation of monomeric A $\beta$ 40 solution from which various dilutions of 5 to 250 nM were made for SPR kinetic analysis. The size exclusion chromatogram of monomeric Aβ40 was reproducible and very similar to that reported earlier (22), (21). The purified monomer did not show any fluorescence emission to Thioflavin T (THT) excited at 450 nm which demonstrates absence of β-sheet structures. In addition, we did not see any aggregation or fibrillar structure when the monomeric fraction was viewed under electron microscope at high magnification (data not shown).

From the monomeric A $\beta$ 40, the fibrils were grown using the following procedure About 1 mg of A $\beta$ 40 peptide was dissolved in 1 ml of PBS (10 mM phosphate buffer pH 7.4) and then bath sonicated for 40 seconds to get a clear solution. The sample was spun at 14000 rpm for 20 min and filtered through 0.22  $\mu$ m syringe. Then the sample was agitated at 250 rpm on an orbital shaker for 48 hrs at 37°C to form A $\beta$ 40 fibrils. The fibrils grown under these condition show strong fluorescence emission to THT excited at 450 nm and exhibit mature fibrillar structure. The last two C-terminal residues of A $\beta$ 42 make the peptide more hydrophobic and less soluble than A $\beta$ 40. In addition, A $\beta$ 42 is known to forms fibrils rapidly compared to A $\beta$ 40, and hence we restricted our studies only to A $\beta$ 40.

### **Instrumentation and Surface Preparation**

SPR analyses were performed at 25°C using Biacore 3000 optical biosensors with research grade CM5 chips (Biacore, Uppsala, Sweden). IgG4.1, raised against human fibrilar Aβ42, was obtained from Mayo Monoclonal Core Facility as described in Poduslo et al (13). Other anti-amyloid antibodies, 4G8 (SIG-39220; Signet/Covance, Dedham, MA), 6E10 (SIG-39320; Signet/Covance, Dedham, MA), or a β-amyloid 1-40- antibody specific to C-terminal (clone 11A50-B10; SIG-39140; Signet/Covance, Dedham, MA) were purchased from commercial vendors. Carboxymethylated CM5 chips were activated using 0.2 M N-ethyl-N'-(dimethylaminopropyl) carbodiimide (EDC) and 0.05 M N-hydroxysuccinimide (NHS). Pure monoclonal antibodies were immobilized at a density of ~2000 response units (RU) to study their binding kinetics with monomeric Aβ40. A nonspecific antibody (L227- IgG1 kappa antibody produced by mouse myeloma L227, Cat. # HB-96, ATCC, Manassas, VA) was immobilized at similar density over the reference surface in order to control for nonspecific binding. A lower level of sonicated Aβ40 fibrils at a density of 9 or 60 Ru was immobilized to study the antibody binding kinetics with Aβ40 fibrils to minimize avidity effects. The residual activated carboxylic acid groups were quenched by blocking the surface with 1M ethanolamine hydrochloride solution. A plain CM5 surface (flow cell, Fc<sub>1</sub>) which was activated and blocked by ethanolamine was used as a reference surface.

### Kinetic Analysis of Aβ Monomers Binding to Immobilized Antibodies

Binding experiments were performed using HBS-EP buffer (0.01 M HEPES, pH 7.4, 0.15 M NaCl, 3mM EDTA, 0.005% P20) as a running buffer. The binding sensorgrams were recorded by injecting different concentrations of freshly prepared A $\beta$ 40 monomers in HBS-EP buffer for 5 min at a flow rate of 30  $\mu$ l/min over the immobilized antibody surface. The dissociation profile was monitored for 15 min, and then the surface was regenerated with 10 mM glycine HCl at pH 3.0. The activity of the immobilized antibody was not affected by the regeneration condition employed here, and the chips were reusable for further experiments. Before performing the kinetic experiments, the surface antigen binding and regeneration conditions were optimized. To avoid any mass transfer effect, the experiments were performed at high flow rate of 30  $\mu$ l/min at 25°C using freshly prepared A $\beta$ 40 monomers.

### Kinetic Analysis of Antibodies Binding to Immobilized Sonicated Aβ40 fibrils

Antibody kinetics with the Aß fibrils may serve as a good in vitro model for studying the antibody interactions with amyloid plaques. However, the heterogeneous nature of fibrils limits this application in obtaining clean kinetic data. To minimize these complexities, the following procedure was employed-  $A\beta40$  fibrils were grown as described above, and the long fibrils (86 μM) were sonicated in a glass tube using a bath sonicator for 2 min to break them into smaller fibrils. The sonicated fibrils were immobilized over the CM5 chip immediately after the sonication to avoid further aggregation of fibrils. To minimize the avidity effect, the sonicated fibrils were diluted in 10 mM sodium acetate at pH 4.0 and immobilized over the CM5 surface at very low density of 60 RU. This procedure allows the fibrils to spread easily and avoid crowded intermolecular interactions. A 10 µl aliquot of sonicated fibrils were mixed immediately with 200 µl of immobilization buffer (10 mM sodium acetate at pH 4.0), injected over the activated CM5 chip surface at a flow rate of 10 µl/min for 3 min, and then the unreacted carboxyl groups were blocked by ethanolamine. The binding sensorgrams were recorded by injecting antibody (33 to 200 nM) to the immobilized Aβ40 fibril surface for 5 min at a flow rate of 30 µl/min using a reference surface (flow cell 1) which was activated and blocked by ethanolamine. The dissociation profile was monitored for about 15 min, and then the surface was regenerated with 10 mM glycine HCl at pH 1.5 buffer.

### Data analysis

The kinetic constants of binding were obtained using a simple 1:1 Langmuir binding model shown below.

$$Analyte + Ligand \underset{k_d}{\overset{k_a}{\rightleftarrows}} Complex$$

This model assumes the simplest situation of an interaction between analyte and immobilized ligand. The model is equal to the Langmuir adsorption isotherm developed by Irving Langmuir to describe the adsorption of molecules on a solid surface at a fixed temperature ((23)). The SPR raw data was analyzed using BIAevaluation software (Version 3.2) provided by Biacore Inc, Uppsala, Sweden). After subtracting the background responses obtained from the control flow cells, the association and dissociation phases were fitted simultaneously using the global fit option, omitting any noisy data at the beginning and end of the analyte injection. In addition, the calculated affinity constant ( $K_D$ ) obtained from the global fit was further validated by applying equilibrium steady state analysis. The  $K_D$  values calculated from both the methods matched closely. However, the global fit did not work well with the data obtained from immobilized A $\beta$ 40 fibrils. Hence, local fit was employed at each concentration and the average kinetic constants were reported in the Table 1.

## Labeling of Amyloid Plaques in APP Mouse and Human AD Brain Sections with IgG4.1, plgG4.1, F(ab')<sub>2</sub>4.1, and pF(ab')<sub>2</sub>4.1

The polyamine (p) modification of IgG4.1 and F(ab')<sub>2</sub>4.1 was performed as described in Poduslo et al. (13). IgG4.1, pIgG4.1, F(ab')<sub>2</sub>4.1, or pF(ab')<sub>2</sub>4.1 was incubated in vitro with cryosections of brain from a 20-month old APP transgenic mouse to test the ability of the antibodies to bind to amyloid plaques. The presence of the immunoglobulin or fragments was detected following the immunoperoxidase method developed to minimize nonspecific binding of mouse monoclonal antibodies in mouse tissue (M.O.M. Peroxidase Kit; PK-2200; Vector Labs, Burlingame, CA). Briefly, fifteen-micron-thick cryosections were lightly fixed with neutral-buffered, 10% formalin for 5 min to prevent the tissue from disintegrating during the two day procedure. The sections were then washed with tap water three times for 5 min each and then twice with 0.3% Triton X-100 in PBS (PBST) for 5 min each. The endogenous peroxidase activity in the tissue was blocked by reacting with 0.3% H<sub>2</sub>O<sub>2</sub> in PBST for 30 min. The sections were rinsed twice in PBST for 5 min each and then blocked for 60 min with M.O.M. blocking solution in PBST according to the instructions. After rinsing twice in PBST for 5 min each, the sections were equilibrated in M.O.M. diluent (M.O.M. Protein Concentrate in PBST) for 5 min and then incubated with 1.0 or 0.5 μg/ml of the immunoglobulin or fragment in M.O.M. diluent overnight at 4°C. For comparison, three standard anti-amyloid antibodies, 4G8 (SIG-39220; Signet/Covance, Dedham, MA), 6E10 (SIG-39320; Signet/Covance, Dedham, MA), or a  $\beta$ -Amyloid 1-40- antibody specific to C-terminal (clone 11A50-B10; SIG-39140; Signet/Covance, Dedham, MA) were tested at the same dilutions. A control section was incubated in M.O.M. diluent alone without the addition of an antibody. The second day, sections were rinsed twice with PBST for 5 min each and then incubated with the biotinylated horse anti-mouse secondary antibody (M.O.M. Peroxidase Kit) at a dilution of 1:250 for 45 min. After rinsing twice in PBST for 5 min each, sections were incubated with ABC reagent (M.O.M. Peroxidase Kit) for 45 min and then rinsed twice in PBS (minus 0.3% Triton X-100) for 5 min each. Sections were reacted with Vector VIP peroxidase substrate (SK-4600, Vector Labs, Burlingame, CA) for 1 min and then rinsed three times in tap water for 5 min each. Sections were rinsed three times in deionized water for 5 min each and then dehydrated with successive changes of ethanol and xylene and then cover slipped. As a control for the effects

of polyamine modification on the binding of the antibodies and fragments to amyloid plaques and brain tissue, a nonspecific antibody (an anti-human Ia antigen IgG1kappa antibody produced by mouse B lymphocyte hybridoma L227, Catalog #HB-96, ATCC), both native and polyamine-modified, was reacted with APP brain sections following the same immunohistochemical procedure described above.

### Densitometry of IgG4.1, pIgG4.1, F(ab')<sub>2</sub>4.1, and pF(ab')<sub>2</sub>4.1 Labeling of Amyloid Plaques in APP Mouse Brain Sections

The intensity of immunoreactivity of the anti-amyloid antibodies was quantitated on amyloid plaques as a measure of affinity. Grayscale images of APP mouse frontal cortex were taken in two hemispheres in two adjacent sections incubated with the anti-amyloid antibodies at two different concentrations. Using image analysis software (Axiovision, Carl Zeiss, Thornwood, NY), the intensity of each plaque was measured. The values were normalized against the background illumination intensity of an ROI measured on the empty slide immediately adjacent to the brain section, expressed as ratios of less than 1.0. Lower intensities and ratios represent darker levels of gray and black and hence higher levels of immunoreactivity and antibody binding

### **RESULTS**

### **Epitope Mapping of IgG4.1**

Surface plasmon resonance was used to map the epitope binding region of IgG4.1. Different fragments of A $\beta$  peptides were injected at a concentration of 100 nM for 60 seconds at 30µl/min flow rate over the immobilized IgG4.1 surface. As shown in Fig 1A, IgG4.1 binds specifically to the *N*-terminal A $\beta$  peptides, A $\beta$ 1-15, A $\beta$ 2-10, A $\beta$ 2-7, but not to A $\beta$ 10-15, A $\beta$ 16-30, or A $\beta$ 30-40. The binding of A $\beta$ 1-15, is nearly identical to the binding of A $\beta$ 2-10, whereas A $\beta$ 2-7 shows reduced binding response without altering the shape of the curve. The reduced binding may rise from the mass differences between the peptides. These data reveal that IgG4.1 has an epitope specificity to A $\beta$ (2-10).

### **Kinetics of Ficin Digested Antibody Fragment**

Ficin is an enzyme widely used to cleave antibodies near the hinge region generating F(ab) or  $F(ab')_2$  fragments without affecting the antigen binding regions. IgG4.1 was digested to  $F(ab')_2$  fragment as described by Poduslo et al. (13), and the binding kinetics of both antibodies with monomeric and fibrillar  $A\beta40$  were evaluated. Fig 1B shows the binding of IgG4.1 and  $F(ab')_24.1$  at a single concentration of 200 nM to fibrillar  $A\beta40$ . The binding sensorgrams of IgG4.1 and  $F(ab')_24.1$  to monomeric  $A\beta40$  from 30 to 3000 nM concentrations and their theoretical fit are shown in Fig 1C and D, respectively. The binding kinetics of native antibody and digested antibody fragment  $F(ab')_24.1$  is largely unaltered with the binding regions being well preserved following enzyme digestion. Similarly, the binding of the native IgG4.1 and  $F(ab')_24.1$  fragments to immobilized  $A\beta40$  fibrils showed nearly identical association curves and a slightly faster dissociation profile of  $F(ab')_24.1$  compared to IgG4.1. Our earlier studies have demonstrated poor binding of Fab fragments to  $A\beta$  fibrils or amyloid plaques, whereas IgG4.1 and  $F(ab')_24.1$  showed nearly identical binding to different forms of  $A\beta40$  (13). Hence, Fab fragments were not used in this study.

#### Kinetic Analysis of Aß Monomers Binding to Immobilized Antibodies

To study the binding kinetics of different antibodies to monomeric A $\beta$ 40, the antibodies were immobilized at about 2000 RU density. A nonspecific antibody (L227- IgG1 kappa antibody produced by mouse myeloma L227, Cat. # HB-96, ATCC, Manassas, VA) was immobilized at similar density over the reference surface in order to control nonspecific binding. Fig. 2

depicts the experimental and theoretical fit of binding of different immobilized antibodies and their kinetics of binding. These profiles also show association and dissociation binding kinetics to freshly prepared monomeric A $\beta$ 40 from concentration 5 to 200 nM. The kinetic parameters obtained from the simultaneous 1:1 Langmuir fit of association and dissociation phases of all sensorgrams are given in Table 1. 6E10 and 4G8 which are standard mAbs used in immunohistochemistry, show very different kinetic patterns but similar affinity to soluble monomeric A $\beta$ 40. 4G8 shows a greater ability to bind to monomeric A $\beta$ 40 with higher association rate constant ( $k_a$ ) of  $26.8 \times 10^4 \text{ M}^{-1}\text{s}^{-1}$ , but its immune complex with A $\beta$ 40 tends to dissociate quickly with a low dissociation constant ( $k_d$ ) of  $0.81 \times 10^{-4} \text{ s}^{-1}$ . Moreover, 4G8 antibody shows an affinity of 30.1 nM to monomeric A $\beta$ 40, which is the ratio of dissociation and association rate. In contrast, the antibody 6E10 shows a 22.3 nM affinity with a slower association constant of  $3.8 \times 10^4 \text{ M}^{-1}\text{s}^{-1}$ , but it forms a more stable immune complex than 4G8 and demonstrates a higher dissociation constant of  $8.48 \times 10^{-4} \text{ s}^{-1}$ .

The peptide capturing antibody 11A50 shows nearly similar kinetic pattern to 4G8 with 32.5 nM affinity to monomeric Aβ40 (Fig. 2C, Table 1). Surprisingly, its immune complex with Aβ40 shows weaker stability with quicker dissociation constant,  $k_d=0.80\times 10^{-4} \rm s^{-1}$ . IgG4.1, which is a plaque binding mAb, shows specific binding to Aβ40 but with extremely low affinity of 512 nM (Fig. 2D, Table 1). The binding response at each concentration is also lower compared to other antibodies studied here, and it forms a less stable immune complex with  $k_d\,0.037~\rm s^{-1}$ . F(ab')<sub>2</sub>4.1 of IgG4.1 showed a kinetic profile similar to the native antibody with an affinity of 491 nM.

### Kinetic Analysis of Antibody Binding to Immobilized Sonicated Aβ40 Fibrils

The sonicated A $\beta$ 40 fibrils are not suitable for use as an analyte to inject over the chip surface due to their heterogeneity. Hence, they were immobilized as a ligand over the chip surface using carbodiimide chemistry at low density of 60 RU, and different concentrations of antibodies were injected as analytes at a flow rate of 30 µl/min. Fig 3 A, B, C depicts the A $\beta$ 40 fibril binding sensorgrams of 6E10, IgG4.1, F(ab')<sub>2</sub>4.1, respectively from 33 to 200 nM concentration. The sensorgrams were reproducible at all concentrations studied and there is not much change in the shape of the sensorgrams. However, the plaque binding antibodies IgG4.1 and F(ab')<sub>2</sub>4.1 show enhanced binding to the fibrils compared to other antibodies studied. In addition, the sensorgrams of IgG4.1 and F(ab')<sub>2</sub>4.1 are nearly similar except that F(ab')<sub>2</sub>4.1 shows slightly quicker dissociation phase. Surprisingly, the peptide capturing antibody 11A50 did not show any reliable binding to the fibrils, which indicates the C-terminal region of fibrillar A $\beta$ 40 may be buried inside the  $\beta$ -sheet fibril structure and hence unavailable for the antibody 11A50. Alternatively, being a peptide capturing antibody, it may have weak affinity to the fibrils.

The carbodiimide chemistry that was employed to immobilize the A $\beta$ 40 fibrils to the dextran matrix of the chip modifies the free NH<sub>2</sub> group from the N-terminal region and also the side chain lysine at positions 16 and 28 of A $\beta$ 40 fibrils. The absence of 4G8 binding to the immobilized A $\beta$ 40 fibrils might be due to the covalent modification at position 16, which could potentially block the epitope binding region of 4G8. The bar chart in Fig 3D shows the peak binding response of different antibodies binding to immobilized sonicated A $\beta$ 40 fibrils at the end of the sample injection (220 sec). Clearly the 6E10 and IgG4.1 antibodies, which are specific to the *N*-terminal region of A $\beta$  peptide show better binding. The plaque binding antibody IgG4.1 and its F(ab')<sub>2</sub>4.1 fragment show greater binding than 6E10. Similar results were also observed when immobilizing very low density (~9 RU) of sonicated A $\beta$ 40 fibrils (data not shown). L227, which is a nonspecific (negative control) antibody, did not show any measurable binding response to A $\beta$ 40 fibrils. Since the shapes of the sensorgrams are nearly

similar, kinetic analysis of these sensorgrams yields comparable affinity constants between 1 to 2.5 nM and nearly similar dissociation constants (Table 1).

Interaction of the injected antibody with the immobilized antigen involves some avidity effect in addition to the specific binding. If there is no avidity effect, injection of the antibodies to the immobilized monomeric A $\beta$ 40 surface and *vice versa* should provide similar kinetics as shown in Fig 2. To evaluate this, we immobilized the monomeric A $\beta$ 40 at a ligand density of 60 RU and injected the chosen antibodies at a concentration of 67 nM (Fig 3E). The sensorgrams were different than those shown in Fig 2, which is most likely due to avidity. The binding response shown in Fig 3F illustrates some interesting trends with the peptide capturing antibody 11A50, which had the most avidity to monomeric A $\beta$ 40 followed by 6E10 and IgG4.1. Being a plaque binding antibody, the avidity of IgG4.1 or F(ab')<sub>2</sub>4.1 is low; they bind to the monomeric A $\beta$ 40 and tend to dissociate quickly compared to 11A50 and 6E10.

The polyamine modification strategy has been employed to increase the BBB permeability of therapeutic or diagnostic proteins delivered to the brain (12-14). In order to study how the modification alters the antigen binding ability, pIgG4.1 or pF(ab')<sub>2</sub>4.1 were injected over the immobilized sonicated Aβ40 chip surface at different concentrations ranging from 33 to 200 nM. Clearly pIgG4.1 (Fig. 5A) and pF(ab')<sub>2</sub>4.1 (Fig 5B) show enhanced binding to sonicated fibrils, as compared to the unmodified IgG4.1 and F(ab')<sub>2</sub>4.1 (Fig. 3). Kinetic analysis of the sensorgrams demonstrates that the affinity constant (K<sub>D</sub>) is not substantially altered compared to the unmodified IgG4.1 and F(ab')<sub>2</sub>4.1 (see Table 1). The perceived change in the K<sub>D</sub> arises from the small changes observed in the association (k<sub>a</sub>) and dissociation (k<sub>d</sub>) constants. In the case of IgG4.1, the polyamine modification increases the association rate from 18.5 × 10<sup>4</sup> to 28.7 × 10<sup>4</sup> (M<sup>-1</sup>s<sup>-1</sup>) without significant change in the dissociation rate. However, with pF (ab')<sub>2</sub>4.1 the association rate decreased from 22.4 × 10<sup>4</sup> to 15.8 × 10<sup>4</sup> (M<sup>-1</sup>s<sup>-1</sup>), and the dissociation rate decreased from 5.34 × 10<sup>-4</sup> to 3.35 × 10<sup>-4</sup> (s<sup>-1</sup>). Since both IgG4.1 or F (ab')<sub>2</sub>4.1 shows weak affinity to monomeric Aβ40, we did not further study the binding kinetics of pIgG4.1 and pF(ab')<sub>2</sub>4.1 to monomeric Aβ40.

## Labeling of Amyloid Plaques in APP Mouse Brain Sections with 6E10, 4G8, IgG4.1, F (ab')<sub>2</sub>4.1, plgG4.1, pF(ab')<sub>2</sub>4.1, L227

The plaque labeling of different anti-amyloid antibodies 6E10, 4G8, IgG4.1,  $F(ab')_24.1$ , and L227 in APP transgenic mouse brain sections is illustrated in Fig. 4. Fifteen-micron sections of APP mouse brain were incubated with anti-amyloid antibodies at 1 µg/ml or 0.5 µg/ml. The plaque labeling increased with increasing antibody concentrations from 0.5 to 1 µg/ml. The antibody 11A50 exhibited much lower immunoreactivity than the other antibodies (Fig 4E). This is most likely due to the weak affinity to amyloid plaques and also it binds to only  $A\beta1$ -40 while the other antibodies bind to both  $A\beta1$ -40 and  $A\beta1$ -42. The nonspecific control antibody (L227), did not exhibit any binding to amyloid plaques (Fig 4F). Polyamine modification of either IgG4.1 or  $F(ab')_24.1$  did not show a substantial effect on plaque labeling (Fig. 5C and D).

The normalized densitometry of anti-amyloid antibody immunoreactivity to amyloid plaques in APP transgenic mouse brain sections is plotted in Fig. 6. Lower gray scale values and ratios represent darker shades of gray and black due to higher levels of immunoreactivity and antibody binding. The gray scale values were normalized by dividing them by the gray scale value of an ROI measured on the empty slide immediately adjacent to the brain section, resulting in ratios of less than 1. The standard error bars are small because of the large number of plaques analyzed for each antibody. The lower concentration of antibody resulted in lower levels of immunoreactivity, which translated into higher ratios. When the concentration of the antibody was halved, the differences are statistically significant, but the differences in immunoreactivity

are not substantial. This is probably due to the high affinity of the antibodies, which is typical for antibodies in general.

### DISCUSSION

The aim of this study was to investigate the binding kinetics of different anti-amyloid monoclonal antibodies to the monomeric and fibrillar A $\beta$ 40 using surface plasmon resonance technique and their plaque binding ability with transgenic AD mouse brain sections using immunohistochemistry. The motivation here is to understand the various biophysical factors governing the efficacy of anti-amyloid antibodies use for different purposes in Alzheimer's research. The knowledge gained from this study would be helpful in selecting a potential antibody for AD research and /or clinical applications.

The results clearly indicate that the antibodies studied show characteristic binding kinetics to monomeric and fibrillar  $A\beta40$  and an ability to bind amyloid plaques that are germane to the antibody itself. The binding kinetics of various antibodies to Aβ40 monomers followed the Langmuir model although IgG4.1 and F(ab')<sub>2</sub>4.1 showed some degree of heterogeneity with a rapid exponential dissociation phase. However, the kinetics of antibody binding to Aβ40 fibrils is confounded by avidity to obtain true kinetics. The terms affinity and avidity are distinct; affinity refers to the strength of a single interaction and avidity describes the combined strength of multiple interactions between the antibody and antigen. For example, IgM may have low or high affinity depending on the antigen, but its avidity is higher compared to IgG due to the availability of ten binding sites which contrast with the two binding sites of IgG. When IgG mAb is immobilized as a ligand to the sensor surface and monomeric antigen is injected as an analyte, the major interaction could be affinity without substantial avidity effect. However, when the monomeric or heterogeneous antigen is immobilized as a ligand and the IgG is injected as analyte, the interactions with the immobilized antigen involve more avidity. It is conceivable that the simple 1:1 Langmuir model may not adequately reflect the multiphasic binding kinetics between Aβ protein and the antibodies. Most of these multiphasic interactions could emerge from the interactions between neighboring antibodies from the sensor surface or due to increased analyte concentrations. To reduce the impact of the multiphasic interactions, we immobilized a low density of ligands on the chip surface and also used low analyte concentrations. As a result, the Langmuir model fit the data reasonably well with good residual plots and acceptable X<sup>2</sup> values. Use of other complex models available in Bio-evaluation software did not improve the fit significantly.

IgG4.1 is a novel plaque binding monoclonal antibody, raised against the fibrillar human A $\beta$ 42 to target AD amyloid plaques for imaging and therapeutic purposes of AD. The IgG4.1 shows more avidity to A $\beta$ 40 fibrils and labels dense core plaques, but shows less affinity (~512 nM) to soluble monomeric A $\beta$ 40. Ficin enzyme digestion of IgG4.1 to F(ab')<sub>2</sub>4.1 did not affect the antigen binding regions. Earlier, we (13) reported that the polyamine modification of IgG4.1 or F(ab')<sub>2</sub>4.1 increases the BBB permeability by ~50 and ~25 fold, respectively. In addition, we have successfully targeted the amyloid plaques by intravenous administration of pIgG4.1 and pF(ab')<sub>2</sub>4.1 in AD transgenic animal. We found that the native IgG4.1 and pIgG4.1 also label amyloid deposits present in blood vessels. In line with these observations, the affinity constant (KD) of pIgG4.1 and pF(ab')<sub>2</sub>4.1 binding to sonicated A $\beta$ 40 fibrils derived from SPR analysis remains similar to the unmodified IgG4.1 and F(ab')<sub>2</sub>4.1 (Table 1). In addition to the fibril binding, its plaque binding ability in AD transgenic mouse brain sections was also not significantly altered (Fig 5, 6). These data confirm the utility of using pIgG4.1 or pF(ab')<sub>2</sub>4.1 as a plaque targeting antibody for molecular imaging.

Recently, Seubert at al. (11) reported that 3D6, a plaque binding antibody, is effective in reducing amyloid plaque burden in AD mice, whereas m266, a peptide capturing antibody, is

not only ineffective in reducing amyloid plaque burden but also increases vascular amyloid. The same group reported that 3D6 antibody shows 2.4 nM affinity to soluble A $\beta$ 42 determined by surface plasmon resonance studies (24). Our plaque binding antibody IgG4.1 shows preferential affinity to fibrillar A $\beta$ 40 (1.5 nM) than monomeric A $\beta$ 40 (512 nM). It is interesting to compare IgG4.1 antibody to a conformational specific antibody reported by Kayed et al. (25) which was raised similar to IgG4.1 by immunizing with homogeneous A $\beta$ 42 fibrils. Interestingly, this antibody specifically binds to  $\beta$ -sheet fibrillar forms of different amyloidogenic proteins such as A $\beta$ ,  $\alpha$ -synuclin and transthyrin but not to the unstructured monomeric or oligomeric forms in a sequence independent manner.

The peptide capturing antibody, 11A50, which is specific to the C-terminal region of A $\beta40$ , shows 32.5 nM affinity to A $\beta40$  but did not show any specific binding to the immobilized fibrils or to the amyloid plaques in AD mouse brain slices. The poor binding to the fibrils may be due to the burial of A $\beta$  binding site inside the  $\beta$ -sheet fibrillar structure or due to the low levels of A $\beta40$  present in mouse tissue sections. In contrast, m266 is another peptide capturing antibody with high  $k_a$  of  $3.1 \times 10^7$  M<sup>-1</sup>sec<sup>-1</sup>,  $k_d$  of  $0.9 \times 10^{-4}$  sec<sup>-1</sup> and extremely high affinity of 2.8 pM to soluble A $\beta$  peptide (26). There are several peptide capturing mAbs that are commercially available for basic science, but it is beyond the scope of this study to compare and contrast their biophysical properties with 11A50. It is certainly beneficial to know the affinity of the antibodies so that an appropriate antibody can be chosen to suit the bioanalytical experiment. While m266 is not commercially available, for example, comparing the affinity of 11A50 and m266, the high affinity of m266 (2.8 pM) to soluble A $\beta$  peptide makes it a better choice than 11A50 to capture soluble A $\beta$  from complex biological samples.

6E10 and 4G8 are standard monoclonal antibodies used in immunohistochemistry for dense core and diffuse plaque labeling, respectively. In addition, these antibodies are also widely used for Aß peptide capturing in various bioanalytical experiments such as ELISA, Western blot, immunoprecipitation, etc. Recently, it was reported that the dense core plaques have more fibrillar structure with  $\beta$  sheet secondary structures, whereas the diffuse plaques are amorphous deposits without any ordered structure (27). The affinity of 6E10 and 4G8 to Aβ40 is nearly similar, but both show different kinetics as shown in Fig 2. Immunohistochemistry followed by densitometry analysis of the plaque labeling shows that 6E10 and IgG4.1 bind to plaques equally well. While the fibril binding kinetic data of 4G8 is hard to obtain from the SPR studies due to the chemistry employed to immobilize the fibrils to the chip surface, its immunohistochemistry demonstrates lower plaque binding compared to 6E10 and IgG4.1. The higher  $k_a$  of  $26.8 \times 10^4 \,\mathrm{M}^{-1} \mathrm{s}^{-1}$  for 4G8 binding to monomeric A $\beta$  may be translated to its better binding to diffuse plaques, which has more randomly structured Aß peptides. Similarly, the slower binding of 6E10 ( $k_a$  3.8 × 10<sup>4</sup> M<sup>-1</sup>s<sup>-1</sup>) to monomeric Aβ40 may be responsible for its ability to bind Aβ40 fibrils (Fig. 3), and higher amyloid plaque binding immunoreactivity observed in the densitometry plaque binding analysis (Fig 6). These results also correlate with a recent study, where it has been demonstrated that systemic and prolonged intracerebroventricular administration of 6E10 antibody reduced amyloid plaque burden in old AD transgenic mice brain (28).

Antibody- antigen interactions are highly specific. The  $A\beta$  peptides exist in morphologically different forms such as monomer, oligomer, and fibrils etc. Based on the solid state NMR structure of  $A\beta$  amyloid fibrils, the first 10 residues of  $A\beta40$  are structurally disordered, while residues 12-24 and 30-40 adapt  $\beta$ -strand conformations and form parallel  $\beta$ -sheets through intermolecular hydrogen bonding (4). It can be said based on this structural model, that IgG4.1 was raised against the flexible region of fibrillar  $A\beta$  peptide. In addition, the epitope region of IgG4.1,  $A\beta2$ -10, also overlaps the immunodominant region AEFRHD of  $A\beta2$ -7. Interestingly, a Blast search of entire human genome with AEFRHD provides amyloid precursor protein as the only hit which has the same sequence. Also when AD patients were actively immunized

with fibrillar  $A\beta42$  peptides with adjuvants, the patients produced polyclonal antibodies which are predominantly specific to the amino terminus of  $A\beta$  peptide (29). Thakker et al (28) reported that  $A\beta$  binding properties of these antibodies are similar to 6E10, but there is not much information available. Understanding the kinetic details of those endogenous polyclonal antibodies may provide critical information on the development of a valid antibody for AD passive immunotheraphy. Recently, Shankar et al. (5) reported that only the antibodies specific to the amino terminus, and not to the C-terminus of  $A\beta$ , are effective in preventing long term potentiation and long term depression of neurons in AD mouse hippocampal slices when the antibodies were coinjected with the toxic  $A\beta$  oligomers isolated from the AD human brain.

Clearly there has been good progress in AD passive immunization research which is moving forward with more focus on N-terminal monoclonal antibodies raised against the N-terminal region of amyloid peptides. While 3D6 and m266 were raised by immunizing covalently coupled  $A\beta$  fragments to sheep anti-mouse IgG, IgG4.1 and the conformational specific antibody discussed above were developed by immunizing Aβ42 fibrils alone. The antibodies IgG4.1 and 6E10 bind specifically to the N-terminal region of Aβ peptide, and both the antibodies bind to monomeric as well as fibrillar Aβ40 (Fig. 2, Fig. 3 and Fig 6). This bivalent binding may be due to the availability of N-terminal region of A $\beta$  peptide in different conformations. In addition, the affinity to monomeric Aβ40 is significantly higher for 6E10 than IgG4.1. A single peripheral administration of 3D6 plaque binding antibody in transgenic mice increased plasma Aβ40-42 levels by 6-9 fold, whereas with the peptide capturing antibody, m266, increased plasma Aβ levels dramatically by 80-100 fold. Similarly, with 6E10, an approximately 6-7 fold increase in plasma Aß peptides has been documented (28),(30). It will be useful to conduct similar studies with IgG4.1, which has low affinity to monomeric Aβ40, but more avidity to fibrillar Aβ40 and develop a predictive pharmacodynamic model by combining the kinetic constants obtained from surface plasmon resonance with the pharmacodynamic response of single peripheral antibody administration. Increasing the antibody delivery across the BBB even by trace amounts without affecting the antigen binding properties by the polyamine modification strategy might increase the therapeutic or diagnostic potential of the antibody (13). In brief, antibodies remain an indispensible tool for both basic and clinical AD research, hence new and faster ways are required to screen antibodies for specific uses. As demonstrated in this study, surface plasmon resonance and immunohistochemistry may provide a rationale to screen potential anti-Aβ mAbs for various purposes.

### REFERENCES

- 1. Selkoe DJ. Alzheimer's disease: genes, proteins, and therapy. Physiol Rev 2001;81:741–766. [PubMed: 11274343]
- Paravastu AK, Leapman RD, Yau WM, Tycko R. Molecular structural basis for polymorphism in Alzheimer's beta-amyloid fibrils. Proc Natl Acad Sci U S A 2008;105:18349–18354. [PubMed: 19015532]
- Petkova AT, Leapman RD, Guo Z, Yau WM, Mattson MP, Tycko R. Self-propagating, molecular-level polymorphism in Alzheimer's beta-amyloid fibrils. Science 2005;307:262–265. [PubMed: 15653506]
- 4. Tycko R. Molecular structure of amyloid fibrils: insights from solid-state NMR. Q Rev Biophys 2006;39:1–55. [PubMed: 16772049]
- Shankar GM, Li S, Mehta TH, Garcia-Munoz A, Shepardson NE, Smith I, Brett FM, Farrell MA, Rowan MJ, Lemere CA, Regan CM, Walsh DM, Sabatini BL, Selkoe DJ. Amyloid-beta protein dimers isolated directly from Alzheimer's brains impair synaptic plasticity and memory. Nat Med 2008;14:837–842. [PubMed: 18568035]

 Lesne S, Koh MT, Kotilinek L, Kayed R, Glabe CG, Yang A, Gallagher M, Ashe KH. A specific amyloid-beta protein assembly in the brain impairs memory. Nature 2006;440:352–357. [PubMed: 16541076]

- 7. Bard F, Cannon C, Barbour R, Burke RL, Games D, Grajeda H, Guido T, Hu K, Huang J, Johnson-Wood K, Khan K, Kholodenko D, Lee M, Lieberburg I, Motter R, Nguyen M, Soriano F, Vasquez N, Weiss K, Welch B, Seubert P, Schenk D, Yednock T. Peripherally administered antibodies against amyloid beta-peptide enter the central nervous system and reduce pathology in a mouse model of Alzheimer disease. Nat Med 2000;6:916–919. [PubMed: 10932230]
- Foster JK, Verdile G, Bates KA, Martins RN. Immunization in Alzheimer's disease: naive hope or realistic clinical potential? Mol Psychiatry. 2008
- 9. Nitsch RM, Hock C. Targeting beta-amyloid pathology in Alzheimer's disease with Abeta immunotherapy. Neurotherapeutics 2008;5:415–420. [PubMed: 18625453]
- 10. DeMattos RB, Bales KR, Cummins DJ, Dodart JC, Paul SM, Holtzman DM. Peripheral anti-A beta antibody alters CNS and plasma A beta clearance and decreases brain A beta burden in a mouse model of Alzheimer's disease. Proc Natl Acad Sci U S A 2001;98:8850–8855. [PubMed: 11438712]
- 11. Seubert P, Barbour R, Khan K, Motter R, Tang P, Kholodenko D, Kling K, Schenk D, Johnson-Wood K, Schroeter S, Gill D, Jacobsen JS, Pangalos M, Basi G, Games D. Antibody capture of soluble Abeta does not reduce cortical Abeta amyloidosis in the PDAPP mouse. Neurodegener Dis 2008;5:65–71. [PubMed: 18182780]
- 12. Ramakrishnan M, Wengenack TM, Kandimalla KK, Curran GL, Gilles EJ, Ramirez-Alvarado M, Lin J, Garwood M, Jack CR Jr. Poduslo JF. Selective contrast enhancement of individual Alzheimer's disease amyloid plaques using a polyamine and Gd-DOTA conjugated antibody fragment against fibrillar Abeta42 for magnetic resonance molecular imaging. Pharm Res 2008;25:1861–1872. [PubMed: 18443900]
- Poduslo JF, Ramakrishnan M, Holasek SS, Ramirez-Alvarado M, Kandimalla KK, Gilles EJ, Curran GL, Wengenack TM. In vivo targeting of antibody fragments to the nervous system for Alzheimer's disease immunotherapy and molecular imaging of amyloid plaques. J Neurochem 2007;102:420– 433. [PubMed: 17596213]
- 14. Poduslo JF, Curran GL, Berg CT. Macromolecular permeability across the blood-nerve and blood-brain barriers. Proc Natl Acad Sci U S A 1994;91:5705–5709. [PubMed: 8202551]
- Abdullah L, Paris D, Luis C, Quadros A, Parrish J, Valdes L, Keegan AP, Mathura V, Crawford F, Mullan M. The influence of diagnosis, intra- and inter-person variability on serum and plasma Abeta levels. Neurosci Lett 2007;428:53–58. [PubMed: 17964720]
- Ertekin-Taner N, Younkin LH, Yager DM, Parfitt F, Baker MC, Asthana S, Hutton ML, Younkin SG, Graff-Radford NR. Plasma amyloid beta protein is elevated in late-onset Alzheimer disease families. Neurology 2008;70:596–606. [PubMed: 17914065]
- 17. Ringman JM, Younkin SG, Pratico D, Seltzer W, Cole GM, Geschwind DH, Rodriguez-Agudelo Y, Schaffer B, Fein J, Sokolow S, Rosario ER, Gylys KH, Varpetian A, Medina LD, Cummings JL. Biochemical markers in persons with preclinical familial Alzheimer disease. Neurology 2008;71:85–92. [PubMed: 18509095]
- Agyare EK, Curran GL, Ramakrishnan M, Yu CC, Poduslo JF, Kandimalla KK. Development of a smart nano-vehicle to target cerebrovascular amyloid deposits and brain parenchymal plaques observed in Alzheimer's disease and cerebral amyloid angiopathy. Pharm Res 2008;25:2674–2684. [PubMed: 18712585]
- Hsiao K, Chapman P, Nilsen S, Eckman C, Harigaya Y, Younkin S, Yang F, Cole G. Correlative memory deficits, Abeta elevation, and amyloid plaques in transgenic mice. Science 1996;274:99– 102. [PubMed: 8810256]
- 20. Wengenack TM, Whelan S, Curran GL, Duff KE, Poduslo JF. Quantitative histological analysis of amyloid deposition in Alzheimer's double transgenic mouse brain. Neuroscience 2000;101:939–944. [PubMed: 11113343]
- 21. Bitan G, Teplow DB. Preparation of aggregate-free, low molecular weight amyloid-beta for assembly and toxicity assays. Methods Mol Biol 2005;299:3–9. [PubMed: 15980591]
- 22. Nichols MR, Moss MA, Reed DK, Lin WL, Mukhopadhyay R, Hoh JH, Rosenberry TL. Growth of beta-amyloid(1-40) protofibrils by monomer elongation and lateral association. Characterization of

- distinct products by light scattering and atomic force microscopy. Biochemistry 2002;41:6115–6127. [PubMed: 11994007]
- 23. Langmuir I. The adsorption of gases on plane surfaces of glass, mica and platinum. J. Am. Chem. Soc 1918;40:1361–1404.
- Tsurushita, N.; Vasquez, MJ. Humanized anti-beta antibodies. Eli Lilly and Company; Indianapolis, IN US, USA: 2008.
- 25. Kayed R, Head E, Sarsoza F, Saing T, Cotman CW, Necula M, Margol L, Wu J, Breydo L, Thompson JL, Rasool S, Gurlo T, Butler P, Glabe CG. Fibril specific, conformation dependent antibodies recognize a generic epitope common to amyloid fibrils and fibrillar oligomers that is absent in prefibrillar oligomers. Mol Neurodegener 2007;2:18. [PubMed: 17897471]
- 26. Davies, J.; Tang, Y.; Watkins, JD. Binding Molecules. USA: 2006.
- Rak M, Del Bigio MR, Mai S, Westaway D, Gough K. Dense-core and diffuse Abeta plaques in TgCRND8 mice studied with synchrotron FTIR microspectroscopy. Biopolymers 2007;87:207–217. [PubMed: 17680701]
- 28. Thakker DR, Weatherspoon MR, Harrison J, Keene TE, Lane DS, Kaemmerer WF, Stewart GR, Shafer LL. Intracerebroventricular amyloid-{beta} antibodies reduce cerebral amyloid angiopathy and associated micro-hemorrhages in aged Tg2576 mice. Proc Natl Acad Sci U S A 2009;106:4501–4506. [PubMed: 19246392]
- 29. Lee M, Bard F, Johnson-Wood K, Lee C, Hu K, Griffith SG, Black RS, Schenk D, Seubert P. Abeta42 immunization in Alzheimer's disease generates Abeta N-terminal antibodies. Ann Neurol 2005;58:430–435. [PubMed: 16130106]
- Gray AJ, Sakaguchi G, Shiratori C, Becker AG, LaFrancois J, Aisen PS, Duff K, Matsuoka Y. Antibody against C-terminal Abeta selectively elevates plasma Abeta. Neuroreport 2007;18:293–296. [PubMed: 17314674]

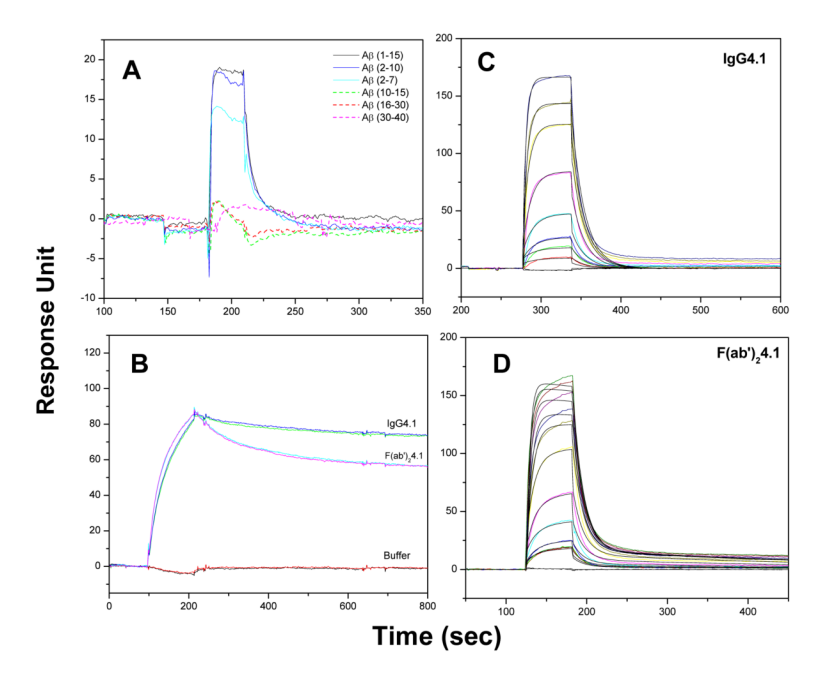


Fig. 1. Epitope mapping of IgG4.1 and kinetics of ficin digested antibody fragment SPR binding sensorgram of IgG4.1 to different A $\beta$  fragments demonstrating the epitope binding region of IgG4.1 as the *N*-terminal region of A $\beta$  peptide from 2-10 (**A**). Binding sensorgram of immobilized fibrillar A $\beta$ 40 binding to IgG4.1 and F(ab')<sub>2</sub>4.1 at 200nM concentration (**B**). Binding sensorgram of immobilized IgG4.1 (**C**) and immobilized F (ab')<sub>2</sub>4.1 (**D**) binding to monomeric A $\beta$ 40 at 30 to 3000 nM concentration. The sensorgrams are shown in color lines and the fits are shown in black lines. This demonstrates that the antibody enzyme digestion to F(ab')<sub>2</sub>4.1 fragments does not alter the binding region.

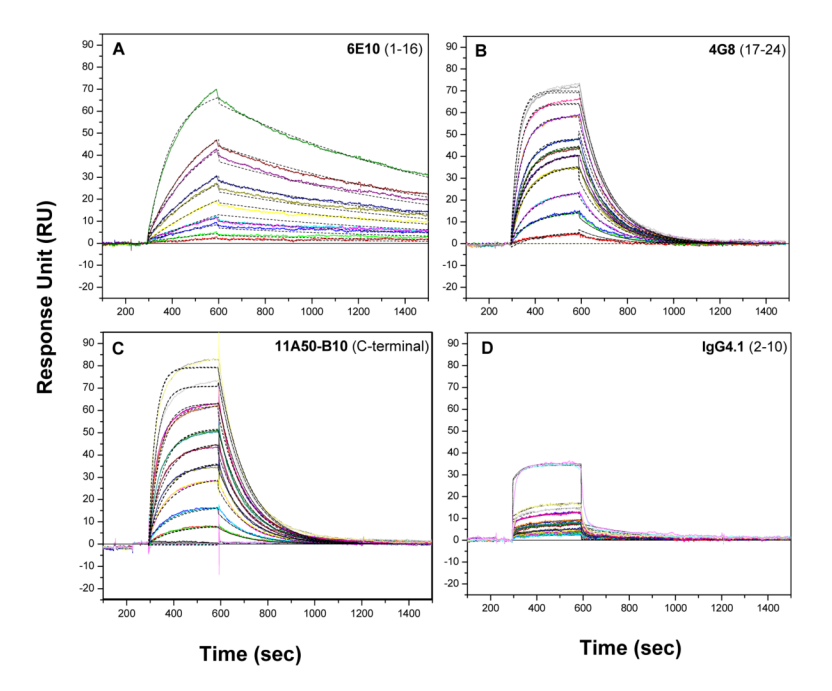


Fig. 2. Kinetic analysis of Aβ monomers binding to immobilized antibodies Kinetic analysis of different immobilized monoclonal antibodies IgG6E10 (A), IgG4G8 (B), IgG11A50 (C), IgG4.1 (D) binding to monomeric Aβ40 at 5, 10, 15, 20, 30, 40, 50, 75, 100, 250 nM concentration. The antibodies were immobilized at a ligand density of about 2000 Ru and monomeric Aβ40 were injected for 5 min followed 15 min dissociation with HBS-EP buffer at 30 μl/min flow rate. The sensorgrams are shown in color lines and the fits are shown in black dashed lines. The kinetic parameters obtained from the fit are shown in the Table 1.

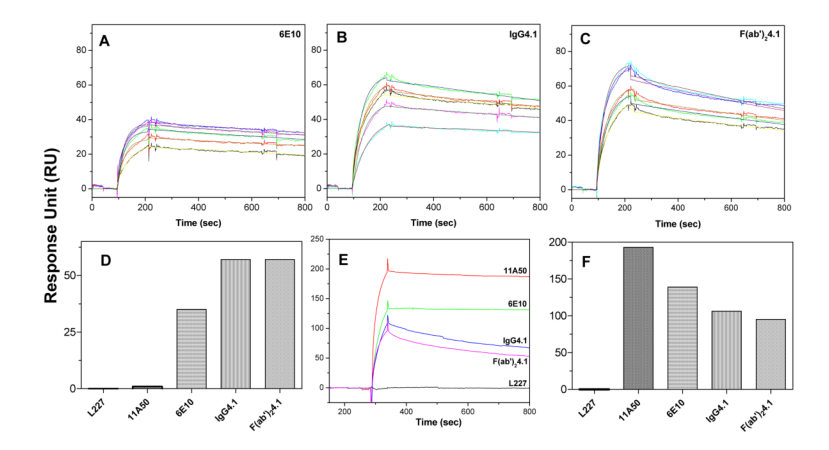


Fig 3. Kinetic analysis of antibody binding to immobilized sonicated Aβ40 fibrils Kinetic analysis of 6E10 (A), IgG4.1 (B), F(ab')<sub>2</sub>4.1 (C), binding to immobilized sonicated Aβ40 fibrils at 33, 66, 100, 166, 200nM concentration. Sonicated Aβ40 fibrils were immobilized at a ligand density of 60 RU and antibody samples were injected for 1 min followed by 15 min dissociation with HBS-EP buffer at 30 μl/min flow rate. The sensorgrams are shown in color lines and the fits are shown in black line. The kinetic parameters obtained from the fit are shown in the Table 1. Panel (D) shows the bar chart of the peak binding response at the end of sample Injection. In panel (E), freshly prepared monomeric Aβ40 was immobilized at a ligand density about 60 RU, and different antibodies were injected at a concentration of 67 nM. Panel (F) shows the bar chart of the peak binding response at the end of sample injection.

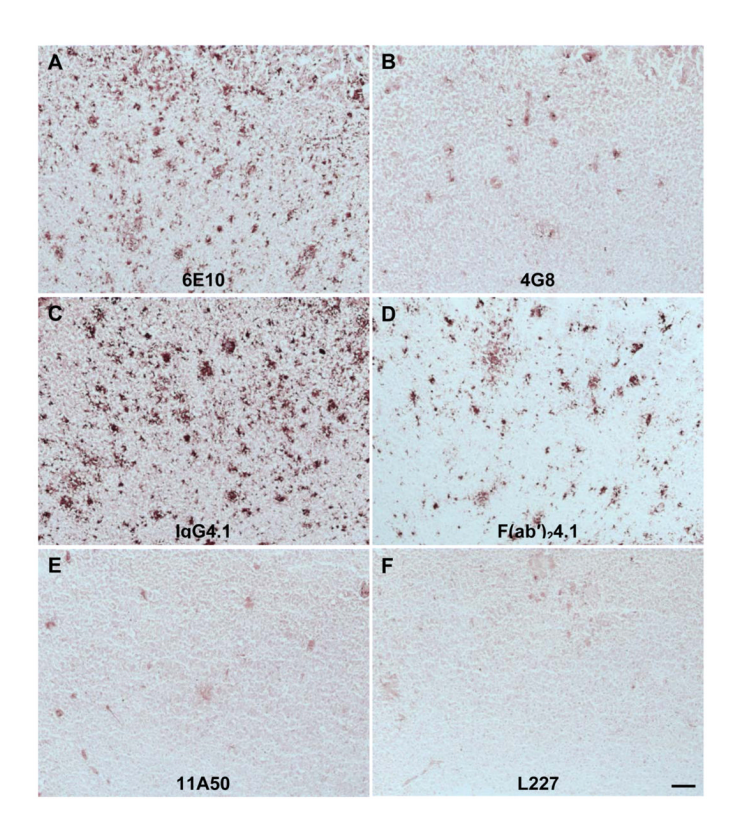


Fig. 4. Labeling of amyloid plaques in APP mouse brain sections with 6E10, 4G8, IgG4.1, F (ab') $_2$ 4.1, and L227

Fifteen-micron sections of APP mouse brain incubated with 1.0  $\mu$ g/ml of the anti-amyloid antibodies are illustrated as follows: (**A**), 6E10; (**B**), 4G8; (**C**), IgG4.1; (**D**), F(ab')<sub>2</sub>4.1; (**E**), 11A50; (**F**), L227. Scale bar equals 100  $\mu$ m.

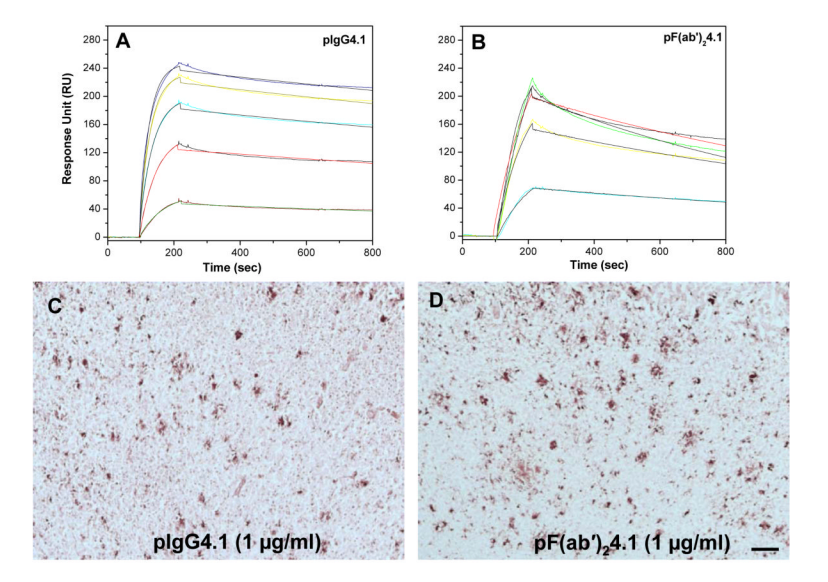


Fig 5. Kinetic analysis of A $\beta$ 40 fibril binding to pIgG4.1 (**A**), pF(ab')<sub>2</sub>4.1 (**B**) at concentrations of 33, 66, 100, 166, and 200nM. Labelling of amyloid plaques in APP mouse brain sections with pIgG4.1 (**C**) and pF(ab')<sub>2</sub>4.1 (**D**). Scale bar equals 100  $\mu$ m.

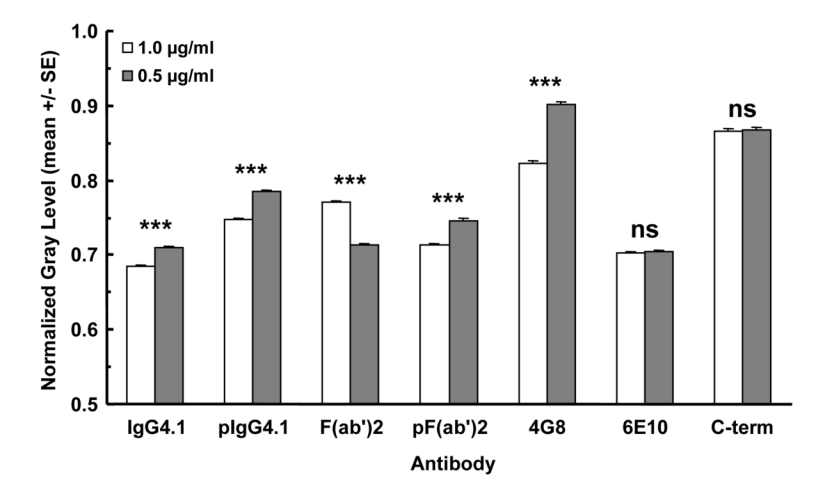


Fig 6. Densitometry of  $6E10, 4G8, IgG4.1, F(ab')_24.1$ , and L227 labeling of amyloid plaques in APP mouse brain sections

The ordinate plots the normalized gray scale values as a mean of the plaques analyzed for each antibody and concentration. The error bars indicate S.E.M. The anti-amyloid antibodies are listed along the abscissa. For each antibody, the left bar represents the 1.0  $\mu$ g/ml concentration and the right bar represents 0.5  $\mu$ g/ml. ANOVA (two-way): Antibody - [F(6,10877)=809.5; p<0.0001]; Concentration – [F(1,10877)=80.52; p<0.0001]; Interaction – [F(6,10877)=73.99; p<0.0001]. Bonferroni post-hoc multiple comparisons: \*\*\* -p<0.0001.

Table 1

Kinetic constants of various antibodies, fragments with monomeric and fibrillar form of  $A\beta40$  obtained from SPR.

Ramakrishnan et al.

${ m Analyte}^{(I)}$ Injected	$ m Ligand^{(2)}$ Immobilized	$k_a(M^{-1}s^{-1})\\ \times 10^4$	$k_d(s^{-1})$	$\begin{array}{c} K_D(M) \\ \times 10^{-9} \end{array}$	Chi <sup>2</sup>
Aβ40 monomer	6E10	3.8	$8.48 \times 10^{-4}$	22.3	1.04
Aβ40 monomer	4G8	26.8	$0.81\times10^{-4}$	30.1	0.81
Aβ40 monomer	11A50	24.7	$0.80\times10^{-4}$	32.5	99.0
Aβ40 monomer	IgG4.1	7.2	0.037	512.0	0.35
Aβ40 monomer	$F(ab')_2 4.1$	3.7	0.018	491.0	2.48
6E10	Aβ40 fibril	20.8	2.91 ×10 <sup>-4</sup>	1.40	2.50
11A50	Aβ40 fibril	No interact	No interaction could be reliably measured	eliably mea	isured
IgG4.1	Aβ40 fibril	18.5	$2.80\times\!10^{-4}$	1.50	6.61
F(ab')24.1	Aβ40 fibril	22.4	$5.34\times10^{-4}$	2.38	3.50
pIgG4.1	Aβ40 fibril	28.7	$2.98\times\!10^{-4}$	1.04	15.40
pF(ab')24.1	Aβ40 fibril	15.8	$3.35 \times 10^{-4}$	2.12	4.49

 $^{(I)}$ Analyte refers to the sample that was injected over the immobilized chip surface.

 $^{(2)}$ Ligand refers to the sample that is covalently linked to the sensor chip surface.

Page 20